

Subcarrier Pairing for Self-Heterodyne OFDM

Nirmal Fernando
ECSE Monash Univ., Australia
Email: Nirmal.Fernando@monash.edu

Yi Hong
ECSE Monash Univ., Australia
Email: Yi.Hong@monash.edu

Emanuele Viterbo
ECSE Monash Univ., Australia
Email: Emanuele.Viterbo@monash.edu

Abstract—In this paper, we present a subcarrier pairing scheme to improve the overall error performance of self-heterodyne (self-het) OFDM communications. The proposed pairing scheme exploits the average signal-to-interference-to noise ratios (SINRs) imbalance experienced among self-het OFDM subcarriers. At the transmitter, two simple operations, symbol constellation rotation and component interleaving, are performed before pairing the *good* and the *bad* OFDM subcarriers, and maximum likelihood detection is used at the receiver to decode the information. The simulation results show that the proposed pairing scheme improves the system performance by 2.5 dB and 0.6 dB for Rayleigh fading and AWGN channels at bit error rate (BER) of 10^{-3} , respectively, without any coding overhead. In addition, we show that, in the presence of phase noise, self-het OFDM using the proposed pairing scheme outperforms the conventional OFDM schemes with superheterodyne receiver structures.

Keywords: Precoding, diversity, OFDM, self-heterodyne, multipath fading, super-heterodyne, non-coherent detection, peak detection, millimeter-wave communication, phase noise, low complexity receivers.

I. INTRODUCTION

Non-congested millimeter-wave and terahertz RF spectra have great potential to be used for high speed data communications [1], [2]. At such high frequencies, the implementation of stable oscillators and carrier phase recovery circuitries are technically challenging. Even using advanced frequency stabilization techniques, phase noise at the receiver is still significant [3]. Thus conventional OFDM schemes that are inherently sensitive to phase noise are impractical for applications in such frequency bands.

To solve this problem, Shoji *et. al.* proposed self-heterodyne OFDM (self-het OFDM)[3], [4] for high-level oscillator instabilities in 60GHz RF band and demonstrated its highly stable performance using a simple RF receiver structure. In self-het OFDM, the transmitter sends both local RF carrier and the OFDM subcarriers. At the receiver, a square-law device or circuitry (self-mixing) is used to down-convert the RF signal without the needs of a local carrier, carrier phase recovery and carrier frequency correction. Since the transmitter can ensure that the local carrier phase is synchronized with the OFDM subcarriers, the self-het OFDM down-conversion is very simple, stable and theoretically has zero phase noise. This advantage comes at the cost of 50% rate reduction.

In this paper, we consider the self-het OFDM and propose a new subcarrier pairing scheme to improve its overall bit error rate (BER) performance over both AWGN and multipath fading channels. Using discrete input alphabets, the

idea of pairing was first presented in [6] for MIMO systems, where channel state information is available at both transmitter (CSIT) and receiver. After using singular value decomposition (SVD) precoding, the MIMO channels are transformed into parallel subchannels. Then the subchannels with good and bad diversity orders are paired together and precoded using signal constellation rotations and component interleaving, which were proved to be robust against the effect of noise [7]. The specific use of component interleaving is to make the real and imaginary components of received symbols experience different fading. If one faces deep fading, the other is still valid. The information theoretic perspective of MIMO pairing using discrete input alphabets was discussed in [8] with practical applications to OFDM. This idea was later extended to optical communications [9].

In this paper, for self-het OFDM, the proposed pairing scheme exploits the unbalanced nature of the signal-to-interference-to noise ratios (SINRs) experienced in the subcarriers. It was shown in our previous work [5] that this property (unbalanced SINRs) holds for self-OFDM over both AWGN and multipath fading channels, respectively. This is due to the intermixing of the noise spectrum with the OFDM subcarriers [4], [5]. Hence, higher-frequency OFDM subcarriers have higher average SINRs, when compared to the lower-frequency ones. Then a subcarrier with high SINR can be paired with one having low SINR, and precoding can be done across each pair of subcarriers. At the receiver, a simple joint maximum likelihood decoding (MLD) is employed to decode each pair of symbols.

We note that the proposed pairing scheme offers three main advantages: (*i*) it involves no coding overhead or increased transmitter power; (*ii*) it has a low decoding complexity, since joint precoding is performed only across a pair of subcarriers; and (*iii*) it improves the diversity order of the system over multipath fading channels.

The paper is organized as follows. In Section II, we review self-het OFDM communications. In Section III, we present the proposed pairing scheme for self-het OFDM. In Section IV, we show the simulation results. Finally, we draw the conclusions in Section V.

Throughout this paper, we adopt the following notation: $\Re\{\cdot\}$ and $\Im\{\cdot\}$ denote real and imaginary components of a complex number, j denotes the imaginary unit, $*$ represents the convolution operation, $\delta(\cdot)$ denotes Dirac Delta function, and G_x represents PSD of signal $x(t)$.

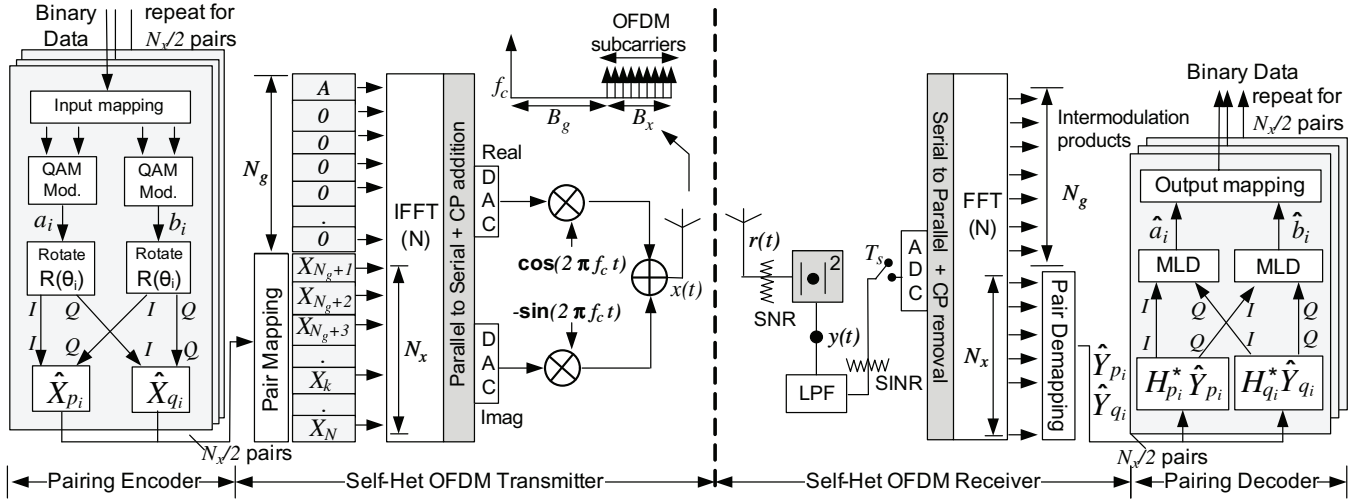


Fig. 1. Self-Het OFDM communication system with proposed pairing scheme

II. SYSTEM MODEL

A. Self-het OFDM

Fig. 1 shows the block diagram of self-het OFDM transceiver, where N , N_x , and N_g represent the size of Inverse Fast Fourier Transform (IFFT), the number of OFDM subcarriers used to encode information, and the number of subcarriers omitted, respectively. At the transmitter, information containing symbols X_k , $k = N_g + 1, \dots, N_g + N_x$, are mapped to the N_x OFDM subcarriers. After the IFFT operation, the time-domain OFDM symbol is generated by adding the cyclic prefix (CP) that has a length sufficient to avoid inter-symbol-interference (ISI). Then, both parallel-to-serial conversion and digital-to-analogue conversion are performed at the transmitter to generate the OFDM signal $s(t)$. Let f_c and Δf denote RF carrier frequency and the OFDM carrier spacing, respectively. The OFDM signal is given by

$$s(t) = \Re \left\{ \sum_{k=1}^{N_x} X_k e^{j2\pi(f_c + B_g + k\Delta f)t} \right\} \quad (1)$$

where $B_g = \Delta f N_g$. The RF signal $x(t)$ can be generated by adding a local RF carrier signal to $s(t)$ with a frequency gap B_g between the carrier and the first OFDM subcarrier, i.e., $x(t) = A \cos(2\pi f_c t) + s(t)$.

If $x(t)$ is transmitted over a multipath fading channel $h(t)$, the received signal is given by $r(t) = h(t) * x(t) + n(t)$, where $n(t) \sim \mathcal{N}(0, \sigma^2)$ is the AWGN noise with the noise power σ^2 . Since the local carrier signal is embedded in the received signal, the non-linear operation $y(t) = |r(t)|^2$ down-converts the passband signal to the baseband signal. We note that the above down-conversion does not require any local carrier generation, carrier phase recovery and carrier frequency correction at the receiver. The power spectral density (PSD)

of $y(t)$ is given by [5], [9]

$$\begin{aligned} G_y(f) &= \underbrace{2\Lambda_c(f) * \{|H(f)|^2 G_s(f)\}}_{\{1\}} \\ &+ \underbrace{\{|H(f)|^2 G_s(f)\} * \{|H(f)|^2 G_s(f)\}}_{\{2\}} \\ &+ \underbrace{G_n(f) * G_n(f)}_{\{3\}} + \underbrace{2\Lambda_c(f) * G_n(f)}_{\{4\}} \\ &+ \underbrace{2\{|H(f)|^2 G_s(f)\} * G_n(f)}_{\{5\}} \\ &+ [\text{DC, } 2f_c \text{ components}]. \end{aligned} \quad (2)$$

where

$$\Lambda_c(f) \triangleq \frac{A^2 |H(f_c)|^2}{4} [\delta(f - f_c) + \delta(f + f_c)]$$

and $G_s(f)$ and $G_n(f)$ represent the PSDs of $s(t)$ and $n(t)$, respectively. The useful OFDM signal component, i.e. the term $\{1\}$ of (2), is generated by mixing the local RF carrier with the OFDM subcarriers. In order to separate the useful term $\{1\}$ from $\{2\}$ in (4), the guard band $B_g = N_g \Delta f$ must satisfy

$$B_g \geq B_x. \quad (3)$$

Hence, the information in $\{1\}$ can be easily recovered at the receiver. Note that the terms $\{3\}$, $\{4\}$ and $\{5\}$ in (2) act as noise and interference impairments. At the receiver, a low pass filter (LPF) with a cutoff frequency $B_g + B_x$ and a DC component filter are used to remove the high frequency and DC components before the sampling and the analog-to-digital conversion (ADC). Then, the CP is removed from the OFDM symbol and the FFT operation is performed after the serial-to-parallel conversion. As shown in Fig. 1, the symbols from last N_x OFDM subcarriers are used for decoding.

B. Equivalent baseband model

The equivalent discrete baseband model of self-het OFDM under multipath fading channels can be written as [5]

$$Y_k = AH_c^* H_k X_k + \hat{Z}_k \quad (4)$$

where H_c , H_k , Y_k and \hat{Z}_k are the equivalent channel response at the local RF carrier, the equivalent channel response at the k -th OFDM subcarrier, the received information symbol at the k -th OFDM subcarrier and the equivalent noise component contributed by the terms {3}, {4}, {5} in (2), respectively. In moderate and high SNR regions, the noise term {3} in (2) insignificant, when compared to the terms {4} and {5}. Hence, the equivalent noise power of the k -th carrier can give be approximated by

$$\sigma_{\hat{Z}_k}^2 = \sigma^2 A^2 \left(|H_c|^2 + \frac{\lambda(k)}{\eta N_x} \right) \quad (5)$$

where

$$\lambda(k) = \frac{2N_x}{N_x + N_g} (N_g + N_x - k)$$

and η denotes the local RF carrier-to-signal power ratio [5]. At the receiver, all channel coefficients can be estimated if a known transmitter symbol pattern (i.e. OFDM training sequence) is transmitted. Hence, the standard channel equalization techniques can be used at the receiver to compensate the frequency selective channel effects.

C. The unbalanced SINRs over OFDM subcarriers

Let γ_k be the instantaneous SINR of the k -th OFDM subcarrier. From (4) and (5), γ_k can be given as

$$\gamma_k = \frac{\eta N_x |H_c|^2 |H_k|^2 \bar{\gamma}}{\eta N_x |H_c|^2 + \lambda(k)} \quad (6)$$

where $k = N_g + 1, \dots, N$ and $\bar{\gamma} = E[|X_k|^2]/\sigma^2$. If we assume that the channel is Rayleigh fading (i.e. $H_c, H_k \sim \mathcal{N}_C(0, 1)$), the expectation of γ_k over channel $\bar{\gamma}_k$, H_c and H_k , can be derived as

$$\bar{\gamma}_k = \bar{\gamma} \left\{ 1 + \frac{\lambda(k)}{\eta N_x} \exp \left(\frac{\lambda(k)}{\eta N_x} \right) \text{Ei} \left[-\frac{\lambda(k)}{\eta N_x} \right] \right\} \quad (7)$$

where $\text{Ei}[\cdot]$ is the exponential integral and it is defined as $\text{Ei}[z] \triangleq -\int_z^\infty \exp(-t)/t dt$. Fig. 2 shows $\bar{\gamma}_k$ at $\bar{\gamma} = 10, 15$ and 20 dBs. We observe that the average SINRs increase, as k increases. This unbalanced SINR scenario motivates us to use the subcarrier pairing, which is described in the following Section.

III. PAIRING OF SELF-HET OFDM

In this section, we present a subcarrier pairing scheme to improve the overall bit error rate (BER) performance of self-het OFDM communications. Since unbalanced SINRs appear in self-het OFDM, the system performance can be improved by using subcarrier pairing. The pairing scheme groups *good* OFDM subcarriers, with high SINRs, and *bad* OFDM subcarriers, with low SINRs. Hence, to improve the overall performance, the self-het OFDM subcarriers located

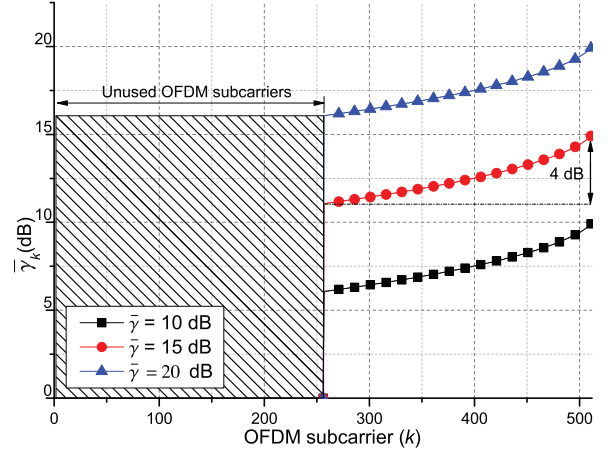


Fig. 2. The variation of average SINRs of subcarriers in self-het OFDM for $\bar{\gamma} = 10, 15$, and 20 dBs. $N = 512$, $N_x = 256$, and $\eta = 1$.

far from the local RF carrier can be paired with those located close to the local RF carrier.

Let $\Phi = \{(a_i, b_i), i = 1, \dots, N_x/2\}$ be the set of M -QAM information symbol pairs transmitted over an OFDM symbol. Each information symbol in the pair (a_i, b_i) is first multiplied by an $\exp(j\theta_i)$ (i.e. θ_i is the rotation angle for the i -th pair) to generate two pre-coded symbols. Subsequently, IQ component interleaving is used over two pre-coded symbols as [7]

$$\begin{aligned} \hat{X}_{p_i} &= \Re\{a_i \exp(j\theta_i)\} + j\Re\{b_i \exp(j\theta_i)\} \\ \hat{X}_{q_i} &= \Im\{a_i \exp(j\theta_i)\} + j\Im\{b_i \exp(j\theta_i)\} \end{aligned} \quad (8)$$

to generate the coded symbol pairs $\Psi = \{(\hat{X}_{p_i}, \hat{X}_{q_i}), i = 1, \dots, N_x/2\}$.

It is shown in [6] how the θ_i 's affect the overall BER of the communication system. Furthermore, the optimum rotation angle θ_i^{opt} depends on the SINR ratio of the OFDM subcarriers that are used to carry $(\hat{X}_{p_i}, \hat{X}_{q_i})$. Let γ_{p_i} and γ_{q_i} be the instantaneous SINRs of OFDM subcarriers, which are used to transmit \hat{X}_{p_i} and \hat{X}_{q_i} , respectively. The *condition number* β_i is then defined as [6]

$$\beta_i \triangleq \sqrt{\frac{\gamma_{q_i}}{\gamma_{p_i}}} \quad (9)$$

The optimal θ_i^{opt} are given in [6] by

$$\theta_i^{\text{opt}} = \begin{cases} \pi/4 & \beta_i \leq \sqrt{3} \\ \tan^{-1} \left\{ \frac{-\sqrt{(\beta_i^2 - 1)^2 - \beta_i^2}}{+(\beta_i^2 - 1)} \right\} & \beta_i > \sqrt{3}. \end{cases} \quad (10)$$

For $i = 1, \dots, N_x/2$, the θ_i^{opt} are computed and used to generate the corresponding coded symbol pairs at the transmitter.

If there is perfect CSIT, the instantaneous SINR (γ_k) is known for each subcarrier. Two optimizations can be performed: (i) selection of the best possible pairing, and (ii) computation of θ_i^{opt} from (9) and (10) of each pair for each channel realization. Let $\Gamma \triangleq [\gamma_{N_g+1}, \dots, \gamma_N]$ be the instantaneous SINRs estimated from (6) for all subcarriers. Then Γ can be sorted in an ascending order and let $\mathcal{I} \triangleq$

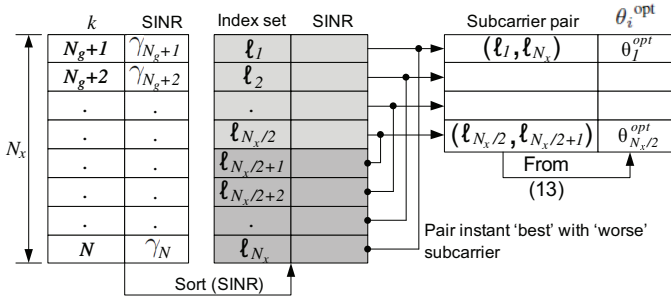


Fig. 3. Selection of best pairs and estimation of θ_i^{opt} if the CSI information is available at the transmitter.

$[\ell_1, \dots, \ell_{N_x}]$ be the index set of the sorted vector. As shown in Fig. 3, at each channel realization, pairing can be performed as $[(\ell_1, \ell_{N_x}), (\ell_2, \ell_{N_x-1}), \dots, (\ell_{N_x/2-1}, \ell_{N_x/2})]$. At the receiver, \mathcal{I} and the selection of correct pairs can be found accordingly.

If there is no CSIT, (i.e., no γ_k), then $\bar{\gamma}_k$ can be used at the transmitter. Hence, for a given OFDM subcarrier pair, the condition number β_i can be estimated by substituting the corresponding average SINRs obtained from (7) into (9) and θ_i^{opt} can be obtained by (10). Since we pair *good* and *bad* subcarriers together, the pair $(\hat{X}_{p_i}, \hat{X}_{q_i})$ is mapped to (X_{N_g+i}, X_{N-i+1}) , where $i = 1, \dots, N_x/2$.

As shown in Fig. 1, demapping the pairs and component deinterleaving are used at the receiver. Then MLD is used to decode the information symbols.

For simplicity of notation, we consider the case with no CSIT. Note that the same technique can be applied to the case with perfect CSIT. Let \hat{H}_{p_i} , where $\hat{H}_{p_i} \triangleq H_c^* H_{N_g+i}$, and \hat{H}_{q_i} , where $\hat{H}_{q_i} \triangleq H_c^* H_{N-i+1}$, be the equivalent channel responses of the $(N_g + i)$ -th and $(N - i + 1)$ -th OFDM subcarriers, respectively. From (4), the received symbols of $(N_g + i)$ -th and $(N - i + 1)$ -th OFDM subcarriers can be written as

$$\begin{aligned}\hat{Y}_{p_i} &= AH_{p_i} \hat{X}_{p_i} + \hat{Z}_{p_i} \\ \hat{Y}_{q_i} &= AH_{q_i} \hat{X}_{q_i} + \hat{Z}_{q_i}.\end{aligned}\quad (11)$$

Then the received information symbols are multiplied by the complex conjugate of corresponding equivalent channel response as

$$\begin{aligned}H_{p_i}^* \hat{Y}_{p_i} &= A|H_{p_i}|^2 \hat{X}_{p_i} + H_{p_i}^* \hat{Z}_{p_i} \\ H_{q_i}^* \hat{Y}_{q_i} &= A|H_{q_i}|^2 \hat{X}_{q_i} + H_{q_i}^* \hat{Z}_{q_i}.\end{aligned}\quad (12)$$

and the MLD is performed to find the decoded information symbols in i -th pair as

$$\begin{aligned}\hat{a}_i &= \arg \min_{X \in \mathcal{X}} \left\{ \begin{array}{l} |\Re\{H_{p_i}^* \hat{Y}_{p_i}\} - A|H_{p_i}|^2 \Re\{X \exp(j\theta_i)\}|^2 \\ + |\Im\{H_{q_i}^* \hat{Y}_{q_i}\} - A|H_{q_i}|^2 \Im\{X \exp(j\theta_i)\}|^2 \end{array} \right\} \\ \hat{b}_i &= \arg \min_{X \in \mathcal{X}} \left\{ \begin{array}{l} |\Im\{H_{p_i}^* \hat{Y}_{p_i}\} - A|H_{p_i}|^2 \Re\{X \exp(j\theta_i)\}|^2 \\ + |\Re\{H_{q_i}^* \hat{Y}_{q_i}\} - A|H_{q_i}|^2 \Im\{X \exp(j\theta_i)\}|^2 \end{array} \right\}\end{aligned}\quad (13)$$

where \mathcal{X} is a QAM constellation.

IV. SIMULATION RESULTS

In this section, we compare self-het OFDM enhanced by pairing (Enhanced self-het OFDM) to the standard self-het

TABLE I
SIMULATION PARAMETERS

Parameter	value
IFFT/FFT size (N)	512
Sampling time (T_s)	$1 \mu s$
Carrier to subcarrier power ratio (η)	0.6
Used & omitted subcarrier (N_x, N_g)	(256, 256)
Channel maximum delay	$64 T_s$
Cyclic prefix (Δ)	$(64 + 1)T_s$
Channel model	Multipath fading, AWGN
Modulation	4-QAM

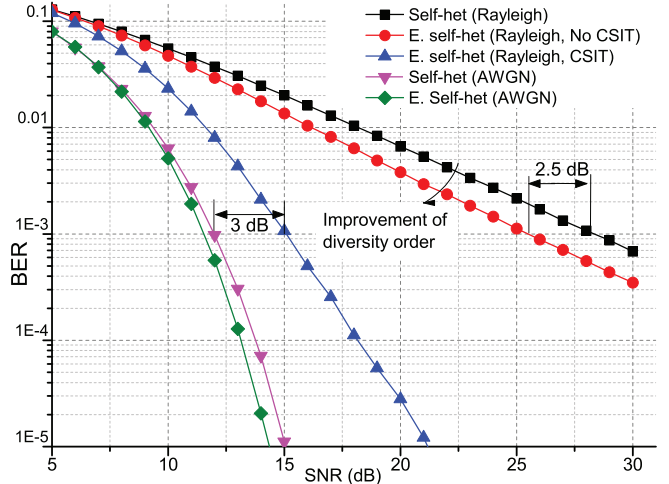


Fig. 4. BER performance improvements of enhanced self-het OFDM for both AWGN and Rayleigh fading channels. 4-QAM signalling. The theoretical BER expression of standard self-het OFDM is given in [5].

OFDM. In both the cases, we incorporate the *smart carrier positioning technique* proposed in [5], which is essential to provide the good performance over multipath fading channels. A summary of key simulation parameters is given in Table I.

Fig. 4 shows the BER performance of enhanced self-het OFDM in both Rayleigh fading and AWGN channel models. In Rayleigh fading, the enhanced self-het OFDM improves the BER performance by approximately 2.5dB at BER of 10^{-3} , when no CSI information available at the transmitter. We observe that the diversity order has also improved in the proposed pairing scheme. In the case of perfect CSI available at the transmitter, the enhanced self-het OFDM improves the diversity order significantly (see Fig. 4) and the BER is within 3dB at 10^{-3} from the corresponding BER over AWGN channels. In AWGN channels, enhanced self-het OFDM scheme offers approximately 0.6dB gain at BER of 10^{-3} . We note that the diversity slopes are non-integer, since the equivalent fading coefficients are not Rayleigh distributed, being the product of two complex Gaussian variables (see (4)).

Fig. 5 compares the BER performance of enhanced self-het OFDM with conventional OFDM schemes with super-heterodyne transceiver structures. We note that the phase noise generated at the transmitter is insignificant, compared to the one generated at the receiver. We adopt the OFDM phase

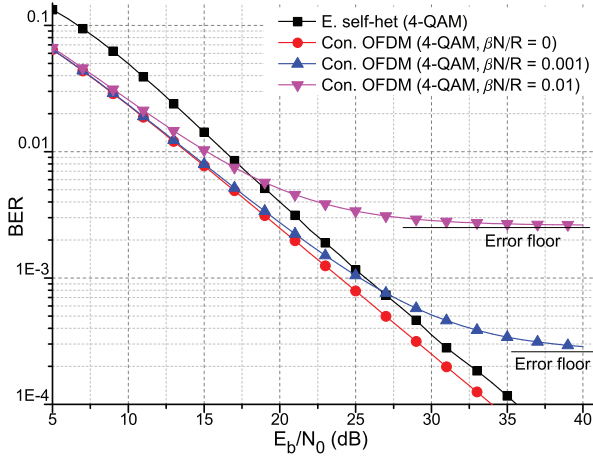


Fig. 5. BER performance of enhanced self-het OFDM and conventional OFDM schemes (superheterodyne transceiver structures) in the presence of phase noise at the receiver. $\beta N/R = 0$ corresponds to no phase noise at the receiver.

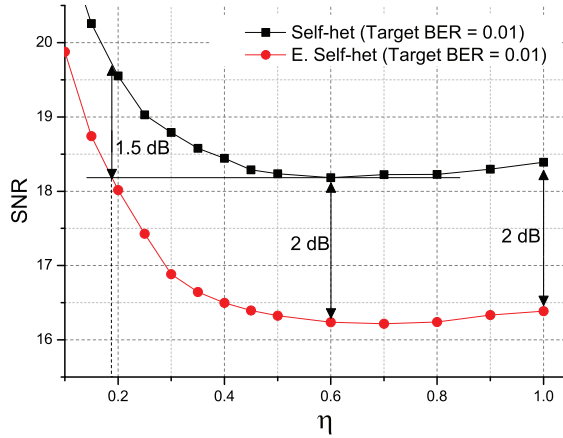


Fig. 6. SNRs, at which the systems can achieve BER of 10^{-2} as a function of η .

noise model proposed in [11] to simulate the phase noise at the receiver. In the presence of phase noise, the BER performance of conventional OFDM schemes (with superheterodyne transceiver structures) reaches an error floor depending upon the level of oscillator instabilities at the receiver. This level of oscillator instabilities is measured by the phase-noise linewidth β , i.e., frequency spacing between 3dB points of its Lorentzian power spectral density function [11]. The simulation results are presented for $N\beta/R = 10^{-3}$ and 10^{-2} , where R is the sampling rate. As shown in Fig. 5, in the presence of high phase noise, self-het OFDM scheme outperforms conventional OFDM schemes with superheterodyne structures at high SNRs, since it does not present an error floor.

Fig. 6 compares the SNRs, at which the systems can achieve BER of 10^{-2} as a function of η (local RF carrier-to-signal power ratio) for Rayleigh fading channels. As the results indicate, the 2dB SNR gain is consistent for $\eta \in (0.4, 1)$, and $\eta \in (0.5, 0.8)$ gives the optimum BER performance for both standard and enhanced self-het OFDMs.

V. CONCLUSION

In this paper, we propose a pairing scheme for self-het OFDM, which improves overall BER performance at very low complexity. At the transmitter, the information symbols are paired and precoded using a constellation rotation and a component interleaver before mapping into OFDM subcarriers with different SINRs. At the receiver, a simple joint MLD can be used for each pair of symbols. For multipath fading channels, if CSIT is available, pairing can be done base on the instantaneous SINRs of the OFDM subcarriers. Without CSIT, pairing is based on the average SINRs at the subcarriers. In both cases, the proposed pairing scheme improves the diversity orders as well as the overall BER performance. Specifically, when there is CSIT, pairing can improve the diversity order significantly and the BER performance is within 3dB at 10^{-3} from the corresponding BER over AWGN channels. Finally, by simulations, we show that self-het OFDM outperforms the conventional OFDM schemes with superheterodyne receivers in the presence of phase noise.

ACKNOWLEDGMENT

This work was performed at the Monash Software Defined Telecommunications Lab and supported by the Monash Professional Fellowship and Australian Research Councils Discovery grant under DP 130100336.

REFERENCES

- [1] P. Smulders, "Exploiting the 60GHz band for local wireless multimedia access: prospects and future directions," *IEEE Comm. Magazine*, vol. 40, no. 1, pp. 140–147, Jan 2002.
- [2] H.-J. Song and T. Nagatsuma, "Present and future of terahertz communications," *IEEE Trans. on Terahertz Science and Tech.*, vol. 1, no. 1, pp. 256–263, Sept. 2011.
- [3] Y. Shoji, M. Nagatsuka, K. Hamaguchi, and H. Ogawa, "60GHz band 64 QAM/OFDM terrestrial digital broadcasting signal transmission by using millimeter-wave self-heterodyne system," *IEEE Trans. on Broadcasting*, vol. 47, no. 3, pp. 218–227, Sept. 2001.
- [4] Y. Shoji, K. Hamaguchi, and H. Ogawa, "Millimeter-wave remote self-heterodyne system for extremely stable and low-cost broad-band signal transmission," *IEEE Trans. on Microwave Theory and Tech.*, vol. 50, no. 6, pp. 1458–1468, June 2002.
- [5] N. Fernando, Y. Hong, and E. Viterbo, "Self-heterodyne OFDM transmission for frequency selective channels," *submitted to IEEE Trans. on Commun.*, 2012.
- [6] S. Mohammed, E. Viterbo, Y. Hong, and A. Chockalingam, "MIMO precoding with X- and Y-codes," *IEEE Trans. on Inf. Theory*, vol. 57, no. 6, pp. 3542–3566, June 2011.
- [7] J. Boutros and E. Viterbo, "Signal space diversity: a power- and bandwidth-efficient diversity technique for the Rayleigh fading channel," *IEEE Trans. on Inf. Theory*, vol. 44, no. 4, pp. 1453–1467, July 1998.
- [8] S. Mohammed, E. Viterbo, Y. Hong, and A. Chockalingam, "Precoding by pairing subchannels to increase MIMO capacity with discrete input alphabets," *IEEE Trans. on Inf. Theory*, vol. 57, no. 7, pp. 4156–4169, July 2011.
- [9] Y. Hong, A. J. Lowery, and E. Viterbo, "Sensitivity improvement and carrier power reduction in direct-detection optical OFDM systems by subcarrier pairing," *Opt. Express*, vol. 20, no. 2, pp. 1635–1648, Jan. 2012.
- [10] Y. Hong, E. Viterbo, and A. J. Lowery, "Improving the sensitivity of Direct-Detection optical OFDM systems by pairing of the optical subcarriers," in *37th European Conference and Exposition on Optical Communications*, Optical Society of America, 2011, pp. Th.11.B.2.
- [11] S. Wu and Y. Bar-Ness, "OFDM systems in the presence of phase noise: consequences and solutions," *IEEE Trans. on Commun.*, vol. 52, no. 11, pp. 1988–1996, Nov. 2004.